HHS Public Access

Author manuscript

J Control Release. Author manuscript; available in PMC 2024 June 01.

Published in final edited form as:

J Control Release. 2023 June ; 358: 729–738. doi:10.1016/j.jconrel.2023.05.029.

Reducing off-target drug accumulation by exploiting a type-III interferon response

Scott G. Tilden[1], **Madison H. Ricco**[1], **Emily A. Hemann**[2], **Thomas J. Anchordoquy**[1]

[1]University of Colorado, Skaggs School of Pharmacy and Pharmaceutical Sciences, University of Colorado Anschutz Medical Campus, Aurora, CO

[2]Ohio State University, Ohio State University College of Medicine, Columbus, OH

Abstract

Nanomedicines have been touted as the future of cancer therapy for decades. However, the field of tumor-targeted nanomedicine has failed to significantly advance toward becoming the primary choice for cancer intervention. One of the largest obstacles that has yet to be overcome is off-target accumulation of the nanoparticles. We propose a novel approach to tumor delivery by focusing on decreasing off-target accumulation of nanomedicines rather than directly increasing tumor delivery. Acknowledging a poorly understood "refractory" response to intravenously injected gene therapy vectors observed in ours and other studies, we hypothesize that virus-like particles (lipoplexes) can be utilized to initiate an anti-viral innate immune response that limits off-target accumulation of subsequently administered nanoparticles. Indeed, our results show a significant reduction in the deposition of both dextran and Doxil® in major organs with a concurrent increase in plasma and tumor accumulation when injection occurred 24 hours *after* a lipoplex injection. Furthermore, our data showing that the direct injection of interferon lambda (IFN-λ) is capable of eliciting this response demonstrates a central role for this type III interferon in limiting accumulation in non-tumor tissues.

Graphical Abstract

To whom correspondence should be addressed: Scott Tilden, 12850 E. Montview Blvd., Skaggs School of Pharmacy and Pharmaceutical Sciences, University of Colorado, Aurora, CO 80045, scott.tilden@cuanschutz.edu, phone: 303-724-6114.

COMPETING INTERESTS: The authors have no competing interests to declare.

CRediT Author Statement:

Scott Tilden: Conceptualization, Methodology, Validation, Formal Analysis, Investigation, Data Curation, Writing – Original Draft, Visualization, Project Administration

Madison Ricco: Investigation, Writing – Review & Editing

Emily Hemann: Resources, Funding Acquisition, Writing – Review & Editing

Thomas Anchordoquy: Resources, Writing – Review & Editing, Supervision, Funding Acquisition

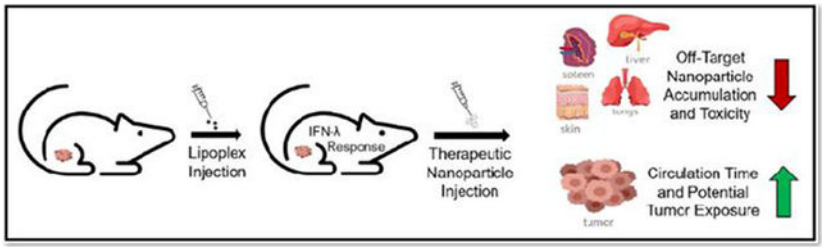

Keywords

Lipoplex; Off-target Accumulation; Immune Response; Cancer; Refractory Response; Tumor Delivery

Introduction:

The field of therapeutic nanomedicines is still attempting to fully characterize and understand the immune responses triggered by intravenous administration of nanoparticles. The most persistent problems the field faces are unintended interactions with the body's milieu, insufficient tumor delivery, and off-target accumulation of nanomedicines in the Mononuclear Phagocytic System (MPS) (a.k.a reticuloendothelial system), which includes the liver, spleen, and other major organs[1-4]. The innate immune system governs the clearance and accumulation of nanomedicines in the MPS and initiates rapid responses to repeat injections of nanomedicines[5-10]. Even with the most promising "stealth" or "targeted" formulations approximately 99% of an injected dose of nanomedicines will accumulate in the MPS and other off-target tissues[11]. Since many chemotherapeutic nanomedicines require repeat injections, this off-target accumulation can lead to altered pharmacokinetics and toxicities that can compromise the therapeutic benefits[12-14]. However, if a reduction in drug exposure in non-tumor tissues could be achieved, it would allow for more aggressive dosing regimens leading to greater therapeutic efficacy. Indeed, the most well-established chemotherapeutic nanomedicine, Doxil® (liposomal encapsulated doxorubicin), has been successful by exploiting a similar strategy. Doxorubicin administered as a free drug is extremely toxic and can cause fatal cardiotoxicity[15]. Doxil® effectively minimizes this cardiotoxicity by reducing off-target doxorubicin accumulation in cardiomyocytes and increasing tumor delivery of doxorubicin[16]. Nonetheless, current research predominantly focuses on "targeting" tumor tissues and "hiding" from the immune system. We suggest that it may be more productive to focus on exploiting the innate immune system to reduce off-target accumulations.

One such immune response that is of particular interest is a poorly understood phenomenon that happens when complexes of nucleic acids and cationic lipids (i.e., lipoplexes) are repeatedly administered (~every 24 hours). Curiously, studies have reported that neither organ accumulation nor expression of the gene therapy vector increases with repeated administrations of lipoplexes, and actually decreases in some cases[9, 10, 17, 18]. This phenomenon was dubbed the "refractory" response, initiating approximately 12 hours after administration and has been reported to last for an average of approximately 2-3 weeks[9, 10, 17, 19-22]. It is understood that this response cannot be due to the complement/antibody

driven Accelerated Blood Clearance (ABC) phenomenon which requires several days to elicit after the initial injection[23]. Additionally, the ABC effect involves an adaptive immune response to PEGylation[23, 24], and not all the nanoparticles in the reported studies were PEGylated. Furthermore, an ABC event would be expected to result in increased hepatic accumulation of the gene therapy vector, which was not observed[6, 7, 25]. Since neither expression nor accumulation of the gene therapy vectors in MPS organs significantly increases with repeated administration, it suggests that the refractory response is an immunological reaction to lipoplexes that directly limits tissue deposition of subsequently administered particles.

When considering the similarities between the structure of viruses and lipoplexes, it is understood why lipoplexes would cause immune reactions. Viruses are on the nanoscale, often possess lipid membranes, have surfaces coated with polysaccharides, and contain DNA/RNA. Similarly, lipoplexes consist of lipid particles that are on the nanoscale, usually contain polyethylene glycol (PEG), which has a similar structure to polysaccharides, and are complexed/conjugated to nucleic acids. Considering these similarities, we propose that the refractory response is an anti-viral response that is triggered when lipoplexes lead to activation of the innate immune system. Recent studies in the field of viral invasion have revealed a novel anti-viral response that provides resistance to viral spread and re-infection[26-35]. This response is rapidly elicited upon sensing of virus-like materials to induce interferons including type III interferons (IFN-λ) produced by epithelial cells, leading to the induction of interferon stimulated genes and a broad anti-viral state within the tissue[28, 36-42]. Additionally, IFN-λ enhances epithelial/endothelial barrier (GI tract, Blood Brain Barrier, Skin) functions, “tightens” cellular junctions, and limits viral invasion and infection of the underlying tissues[27, 29, 31, 35, 39, 43]. We hypothesize that administration of lipoplexes leads to an anti-viral response that systemically tightens healthy epithelium and limits tissue deposition of a subsequently administered particle.

It could be beneficial to tighten the body’s epithelial barriers and limit systemic exposure to potentially toxic particles such as chemotherapeutic nanomedicines. However, chemotherapeutic nanomedicines also need to be delivered to the tumor to be efficacious. In this context, it is well established that the tumor microenvironment is highly dysregulated especially with regards to epithelial structure and immune responses[44-47]. In fact, avoiding immune detection and promoting inflammation are two of the most prominent hallmarks and enabling characteristics of cancers[44]. Due to the dysfunction of the tumor microenvironment, it is likely that tumor tissues will respond differently to a lipoplex injection as compared to healthy tissues. Therefore, if the tumor possesses a compromised ability to properly respond to immunological signals such as IFN-λ, then the tumor microenvironment may remain relatively unaffected during a systemic tightening event. Under such conditions, a dose of nanoparticles administered to a tumor-bearing subject would potentially exhibit reduced particle deposition in healthy tissues while accumulation in the tumor remains unimpeded. This is consistent with our studies on the repeat administration of lipoplexes in tumor-bearing mice[18, 48].

In this study we conducted experiments to characterize the refractory response and determine the organ/tumor accumulation of intravenously injected dextran/Doxil® in mice

that had been pretreated with saline, lipoplexes, liposome, or IFN-λ. We also demonstrate that the refractory response is unique to virus-like particles that contain nucleic acids. Our results clearly illustrate that an IFN-λ response is initiated when lipoplexes are intravenously administered while a liposome treatment does not elicit the production of IFN-λ. Additionally, our data demonstrate that pretreatment with either a lipoplex or IFN-λ leads to a significant *decrease* in organ dextran/Doxil® deposition coupled with an *increase* in plasma and tumor accumulation.

Materials and Methods:

Liposome/Lipoplex Preparation:

Sphingosine, cholesterol, 1,2-diarachidoyl-sn-glycero-3-phosphocholine (DAPC), and C16-PEG750-Ceramide were purchased from Avanti Polar Lipids (Alabaster, AL) and used to prepare liposomes at a 3:2:4.5:0.5 mole ratio (respectively) or a 3:2:5 mole ratio for non-PEGylated liposomes as previously described[49]. The liposome preparations have an average diameter of 135 nm, a polydispersity index (PDI) of 0.137, and were prepared in sterile 5% dextrose to adjust the tonicity of the injection solution. To form lipoplexes, liposomes were mixed with plasmid DNA (donated from Megabios Corp., Burlingame, CA) in sterile 5% dextrose at a charge ratio of 0.5[49, 50]. The resulting lipoplexes have an average diameter of 176 nm and PDI of 0.084. A Malvern Zetasizer Nano-ZS was used for all size measurements. Sterile phosphate buffered saline (PBS; 10 mM phosphate, 137 mM NaCl, 2.7 mM KCl, pH 8.25), lipoplexes [0.075 μmoles of DNA (25 μgrams) complexed with 0.125 μmoles total lipid (0.0375 μmoles sphingosine)], or naked liposomes (0.125 μmoles total lipid) were injected via tail vein as previously described[49]. Particle preparation was performed in a sterile biosafety cabinet.

Animals:

Tumor-Bearing Experiments: Prior to treatment, female immunocompetent Balb/c mice 6–10 weeks old were acquired from Jackson labs (Bar Harbor, ME) and allowed to acclimate for one week. The mice were then inoculated in the right flank with approximately 1 million CT26 murine colon carcinoma cells (ATCC #CRL-2638). Tumors were allowed to grow for approximately 7 days or until tumor size reached at least 100 mm^3. Mice were then randomized into treatment groups standardized to tumor volume. Each mouse received a single dose of 200 μL 1x PBS, 200 μL liposomes, 200 μL lipoplexes (25 μg total DNA, charge ratio 0.5), or 1 or 10 μg of recombinant mouse IFN-λ2 (R&D Systems, 4635-ML-025/CF) in 100 μL 1x PBS by a tail vein injection. Twenty-four hours after pretreatment, animals were administered a 10 mg/kg dose of FITC-dextran (Sigma-Aldrich, FD150S) or 10 mg/kg dose of liposomal doxorubicin (Doxil®; Sun Pharmaceutical Industries) via tail vein. Twenty-four hours after the second injection, animals were euthanized, and organs collected for analysis.

ELISA Experiments: Prior to treatment, female immunocompetent Balb/c mice 6–10 weeks old were acquired from Jackson Labs and allowed to acclimate for one week. Mice were then randomized into treatment groups standardized to body weight. Each mouse received a single dose of 200 μL 1x PBS, 200 μL lipoplexes, or 200 μL liposomes by a tail

vein injection. Twelve, 24, 36, 48, and 72 hours after injections, animals were euthanized, and whole blood collected through cardiac puncture for serum preparation and ELISA analysis. All animal procedures were approved by the University of Colorado Institute for Animal Care and Use Committee in accordance with guidelines from the National Institutes of Health (USA).

Quantification of FITC-Dextran Fluorescence and Dextran Extraction Efficiency:

Fluorescein isothiocyanate (FITC) labeled dextran was chosen for these studies since it is commonly used to quantify endothelial and epithelial cell barrier permeability[49-53,56]. The physical properties of dextran have been extensively characterized, and higher molecular weight dextrans possess progressively larger hydrodynamic diameters[57]. FITC-dextran with a molecular weight of approximately 150 kD was used for these studies, and dynamic light scattering measurements estimate its hydrodynamic diameter at approximately 100 nm (data not shown); consistent with published data approximating the size of various dextrans[57].

A standard curve of fluorescence for the FITC-dextran used in this project was determined through fluorescence measurements of a serially diluted stock solution of the FITC-dextran in 1x PBS. Fluorescence measurements were conducted in a CellStar™ μClear™ 96-Well, Cell Culture-Treated, Flat-Bottom Microplate from Greiner Bio-One™ (Monroe, NC) at an excitation of 490 nm and emission of 520 nm using a Molecular Devices (San Jose, CA) SpectraMax M5. To determine dextran extraction efficiency for each whole organ and tissue (lung, heart, liver, spleen, kidneys, brain, tumor), varying amounts of dextran (i.e., 0, 1, 2, 3, 4, 5 μg) were spiked into sets of blank tissues from untreated mice. The tissues were then processed through the dextran extraction procedure described below. Fluorescence of the extracted material was then measured, and total micrograms of dextran calculated with the fluorescence standard curve. Each extraction from spiked tissues was performed in duplicate. The resulting values were averaged and plotted against the total micrograms of dextran spiked into the tissues to create a standard curve for dextran extraction (included in supplementary materials).

Extraction of FITC-Dextran and Quantification of Organ Accumulation:

Organs collected from animals were immediately flash-frozen in liquid nitrogen and stored at −80 °C until analysis. Organs were thawed, weighed, and extracted using a PBS buffer extraction method. Briefly, each organ was placed in a 2-ml screw cap tube (each liver was equally divided into two tubes) with five 2.3-mm diameter zirconia/silica beads from BioSpec Products (Bartlesville, OK) plus 1 mL of lysis buffer (1x PBS with 1% sodium dodecyl sulfate), and 100 μg Proteinase K from Qiagen (Hilden, Germany) was added to each organ. Organs were then incubated at 55 °C for 1 hour. After incubation, organs were homogenized using a MiniBeadBeater-16 Model 607 from BioSpec Products (Bartlesville, OK) for 3.5 minutes. Once homogenized, 100 μL of 20% w/v trichloroacetic acid was added to the homogenate and samples were vortexed for 10 seconds to precipitate proteins. The homogenate was then centrifuged at ~15,000 RCF for 10 min. The supernatant was aspirated into a new tube (supernatants of the divided livers were combined and total volume brought up to 10 mL with 1x PBS) and solution pH was adjusted to pH 8-9 using 1 M sodium

hydroxide. FITC fluorescence of the extracted solution was then measured, and total dextran accumulation was calculated using the extraction efficiency and standard curves described above (see supplementary materials).

IL28A/B Quantification by ELISA:

Serum was prepared by allowing whole blood to clot at room temperature for 30 minutes. Clotted blood was then centrifuged at 5000 RCF for 15 minutes at 4 °C. Serum was then aspirated into new tubes and frozen at −20 °C. Serum levels of IFN-λ were determined through enzyme-linked immunosorbent assay (ELISA) using the manufacturer's recommendations and protocols. Mouse IL-28A/B (IFN-lambda 2/3) DuoSet® ELISA (DY1789B-05) was purchased from R&D Systems® (Minneapolis, MN).

Quantification of Doxorubicin Fluorescence and Organ Accumulation:

A standard curve of fluorescence for doxorubicin was determined through fluorescence measurements of a serially diluted stock suspension of the Doxil® in 90% isopropyl alcohol (IPA) acidified with HCl to a final concentration of 0.075 M. Fluorescence measurements were conducted in a CellStar™ μClear™ 96-Well, Cell Culture-Treated, Flat-Bottom Microplate from Greiner Bio-One™ (Monroe, NC) at an excitation of 470 nm and emission of 595 nm using a Molecular Devices (San Jose, CA) SpectraMax M5. To determine doxorubicin levels in whole organs and tissues (lung, heart, liver, spleen, kidneys, brain, tumor, skin, plasma), blank tissues were run through an extraction procedure using 90% IPA/0.075 M HCl as described below. Once extracted, the blank organ extract was used as a buffer to serially dilute a stock suspension of Doxil®. The equation from the resulting standard curve of fluorescence from each specific organ was used to calculate the total amount of doxorubicin extracted from a corresponding Doxil®-treated organ.

Extraction of Doxorubicin from tissues:

Organs collected from animals were immediately flash-frozen in liquid nitrogen and stored at −80 °C until analysis. Organs were thawed, weighed, and extracted using a buffer made of 90% IPA/0.075 M HCl. Briefly, each organ was placed in a 2-ml tube containing lysis matrix A (MP Biomedical, 6910500) (each liver was equally divided into four tubes) and 1 mL of 90% IPA/0.075 M HCl was then added to each tube. Organs were then homogenized using a MiniBeadBeater-16 Model 607 from BioSpec Products (Bartlesville, OK). Tubes were shaken for 90 second then allowed to rest on ice for 5 minutes before another 90 second shake. Once homogenized, the tubes were allowed to rest on ice for 5 minutes before being centrifuged at ~15,000 RCF for 15 minutes at 4 °C. The supernatant was aspirated into a new tube and total volumes for all organs, except livers, were standardized to 1 mL using 90% IPA/0.075 M HCl. Divided liver supernatants were added together and standardized to 4 mL using 90% IPA/0.075 M HCl. Doxorubicin fluorescence of the extracted solution was then measured, and total doxorubicin accumulation was then calculated using the doxorubicin fluorescence standard curves described above (see supplementary materials). Based off our own extraction experiments and previous literature, an extraction efficiency of >95% was assumed for all extractions[58].

Statistics:

For all comparisons, an unpaired t-test with Welch's correction was performed using GraphPad Prism version 9.5.0 for Windows, GraphPad Software, San Diego, California USA, www.graphpad.com.

Results:

Effect of Lipoplex Pretreatment on Dextran Accumulation

To assess the effects of a lipoplex pretreatment on dextran accumulation, mice were intravenously injected with either PBS or lipoplexes. Twenty-four hours after pretreatment, a 10 mg/kg dose of FITC-dextran was administered. Twenty-four hours after the dextran administration, tissues were harvested from experimental mice and the total dextran accumulation in tissues was determined using the standard curves described above (see supplementary materials). Our results demonstrate that a lipoplex pretreatment significantly reduces dextran accumulation in liver and spleen when compared to mice pretreated with PBS (Figure 1A&B). We also observe a reduction in dextran accumulation for other major organs (lung, kidney, heart) although these trends are not statistically significant under our experimental conditions (Figure 1D-F). Accumulation in the brain was unaffected (Figure 1G). In contrast to that seen in the major organs, the tumor experienced a significant increase in dextran accumulation when compared to PBS treated mice (Figure 1C).

Altered Dextran Accumulation is Dependent on the Presence of Nucleic Acids in the Pretreatment Injection

To determine if lipid/nucleic acid complexes are the primary driver of the refractory response to lipoplex pretreatment, dextran accumulation in organs and tumor tissues were compared between liposome pretreatment and PBS/lipoplex pretreatment groups. The liposome formulation and sizes were identical to the lipid nanoparticles used to form the lipoplexes and were not complexed with plasmid DNA. The timing of the pretreatment and dextran administrations were the same as described above. Our results show that there are no significant differences in dextran accumulation in the organs and tumor between liposome and PBS pretreatments except in the spleen which exhibited a slight increase for the liposome-treated group (Figure 1A-G). In contrast, lipoplex pretreatment significantly reduced dextran accumulation in the liver and spleen compared to animals pretreated with liposomes (Figure 1A&B). We also observe slightly lower accumulation in the lung, kidneys, heart, and brain from lipoplex-treated animals as compared to those receiving liposome pretreatment, but the differences were not statistically significant. However, dextran accumulation in tumors was significantly increased in lipoplex-treated mice when compared to liposome-treated (Figure 1C).

Effect of Lipoplex Pretreatment on Doxil® Accumulation in Organs and Tissues

To assess the effects of lipoplex pretreatment on Doxil® accumulation, mice were intravenously injected with either PBS, lipoplexes, or non-PEGylated lipoplexes. Twenty-four hours after pretreatment, a 10 mg/kg dose of Doxil® was administered. Twenty-four hours after Doxil® administration, tissues were harvested from experimental mice and

the total Doxil® accumulation in tissues was determined using the extraction method and standard curves described above (see supplementary materials). Our results demonstrate that a lipoplex pretreatment significantly reduces Doxil® accumulation/concentration in all major organs (except liver) and plasma when compared to mice pretreated with PBS (Figure 2 & 3). Surprisingly, the liver showed a slight increase in Doxil® accumulation for lipoplex treated mice (Figure 2B). In contrast, non-PEGylated lipoplex pretreatment significantly reduced Doxil® accumulation in all major organs, including liver, when compared to mice pretreated with PBS (Figure 2). However, the plasma of mice pretreated with non-PEGylated lipoplexes experienced an increase in Doxil® concentration (Figure 3A). Curiously, tumor accumulation appeared to show a slight decrease in accumulation, but the differences were not statistically significant under our experimental conditions (Figure 3B).

Quantification of IFN-λ in Response to Lipoplex/Liposome Treatment

To test our hypothesis regarding whether lipoplex treatment initiates a systemic IFN-λ response and if that response is dependent on the nucleic acid component, female Balb/c mice were injected with lipoplexes, liposomes, or 5% dextrose as a control. Serum was collected from the mice at several time points up to 72 hours. IFN-λ levels in serum were then quantified using an enzyme-linked immunosorbent assay (ELISA). Serum from mice treated with lipoplexes show an average of 153.67 pg/mL of IFN-λ twelve hours after treatment (Figure 4B). Twenty-four hours after lipoplex treatment, serum levels of IFN-λ peak at an average of 201.81 pg/mL (Figure 4B). At 36 hours after lipoplex treatment, serum levels of IFN-λ were detected at an average of 10.40 pg/mL (Figure 4B). However, this is well below the lowest concentration that can be reliably determined by the ELISA (Lower Limit of Quantification (LLoQ) = 31.30 pg/mL). Forty-eight hours after lipoplex treatment only 1 out of 4 mice showed detectable levels of IFN-λ at 119.90 pg/mL (Figure 4B). At the final time point of 72 hours, two out of four mice showed detectable levels of IFN-λ at 40.27 and 49.57 pg/mL (Figure 4B). For liposome and 5% dextrose treatments, no serum samples showed IFN-λ at levels above the LLoQ at any time point (Figure 4C&D).

Effect of IFN-λ Pretreatment on Doxil® Accumulation in Organs and Tissues

Hypothesizing that IFN-λ is primarily responsible for the refractory response we observe, we directly employed this cytokine in further experiments. To assess the effects of IFN-λ pretreatment on Doxil® accumulation, mice were intravenously injected with either PBS, 1 μg of IFN-λ, or 10 μg of IFN-λ. Twenty-four hours after pretreatment, a 10 mg/kg dose of Doxil® was administered intravenously. Twenty-four hours following Doxil® administration, tissues were harvested from experimental mice and the total Doxil® accumulation in tissues was determined using the extraction method and standard curves described above (see supplementary materials). Our results demonstrate that a 10 μg IFN-λ pretreatment significantly reduces Doxil® accumulation in all major organs when compared to mice pretreated with PBS (Figure 5). In contrast to that seen in the major organs, the tumor and plasma experienced an increase in Doxil® accumulation when compared to mice pretreated with PBS. However, the tumor differences were not statistically significant under our experimental conditions (Figure 6).

Doxil® Accumulation Ratios

To determine Doxil® accumulation ratios, plasma and tumor accumulation data was divided by liver accumulation data. Lipoplex pretreatment shows a significant decrease in plasma-to-liver Doxil® accumulation ratio (Figure 7A). In contrast, non-PEGylated lipoplex and 10 μg IFN-λ pretreatment significantly increased the plasma-to-liver Doxil® accumulation ratio (Figure 7A). However, only 1 and 10 μg IFN-λ pretreated tumors showed significant increases in tumor-to-liver accumulation ratios compared to PBS treatment (Figure 7B).

Discussion:

Overcoming clearance by the MPS continues to be a significant barrier to efficient nanoparticle-mediated delivery. To combat these issues researchers have attempted many different approaches that generally focus on targeting tumor tissues and/or hiding from the MPS and immune system. However, these proposed solutions have not had a significant impact on increasing tumor delivery. The average tumor accumulation of almost any given nanoparticle remains at or below 1% of the injected dose[11]. Considering that the primary biological role of the innate immune system and MPS is to detect foreign entities and filter the blood, it is not surprising that this represents a formidable barrier to nanoparticle-mediated delivery. As an alternative to tumor targeting, some studies have attempted to block the uptake capacity of the MPS as a way to reduce off-target accumulation and increase tumor accumulation[59-67]. This approach involves delivering massive doses of nanoparticles intended to saturate the MPS immediately prior to administering the therapeutic nanoparticle. Other studies have gone a step further and completely ablated the Kupffer cell population in the liver to prevent uptake by those cells[68-70]. These approaches may increase tumor delivery of the therapeutic nanoparticle but the clinical utility of saturating or eliminating MPS cells is questionable. Furthermore, the immunological consequences of repeated administrations of the particle used to impose saturation have yet to be fully investigated. It is also worth noting that one of the fundamental goals of nanoparticle-mediated drug delivery is to *reduce* off-target toxicities and exposure. As such, destroying an entire subset of cells or saturating the filtration capabilities of the MPS runs counter to those principles. In contrast, utilizing the immune system's protective abilities to limit MPS uptake would be a less invasive, less toxic, and potentially more efficacious approach than blocking, eliminating, or attempting to hide from the MPS.

Nanoparticle-mediated gene delivery has had to overcome some of the most intriguing and distinct immunological reactions reported in the field of drug delivery. A host of reactions characterized by circulating leukocyte uptake[71], complement and antibody mediated clearance[6, 24, 25, 72], cytokine/chemokine driven inflammation[73, 74], or toxicities caused by cationic lipids have all been reported[49]. However, the poorly understood refractory response to repeat administrations of nonviral vectors is unique in that it specifically reduces the accumulation of a second dose. This is clearly a barrier to achieving therapeutic lipoplex levels in tissues, but this phenomenon could potentially be exploited to reduce off-target accumulation of a nanomedicine. Due to the physicochemical similarities between lipoplexes and viruses, we propose that this refractory response is actually an

anti-viral response that utilizes IFN-λ to protect healthy tissues from viral exposure and infection. In support of the suggestion, the data presented in Figure 4 clearly demonstrate that a lipoplex injection initiates a systemic IFN-λ response. If this IFN-λ response can be triggered before delivery of a chemotherapeutic nanomedicine, our data indicate that off-target accumulation in healthy tissues can be significantly reduced. In the case of Doxil®, it is specifically relevant that accumulation in the skin was reduced because palmar-plantar erythrodysesthesia is known to be a dose-limit clinical toxicity[75].

While the refractory response is known to reduce uptake in healthy tissues, previous studies describing this phenomenon did not include tumor-bearing animals[10, 17, 22]. We believe that the lack of tumor-bearing animals used in those studies combined with the reliance on expression (as opposed to quantifying delivery) allowed the effects reported here to be overlooked. Although many gene delivery studies utilize tumor-bearing models, very few of these studies quantify delivery after repeat administration in immunocompetent animals. Our previous work described non-additive effects of repetitive lipoplex administration wherein delivery to the tumor was enhanced 26-fold as compared to a single dose under conditions where delivery to organs was minimally affected[48]. Our more recent work has also observed this phenomenon after just two injections, and demonstrates that cytokines in the tumor remain very low despite soaring cytokine levels in the major organs[18]. These observations are consistent with the well documented phenomenon of immunosuppression and cellular dysregulation in the tumor microenvironment[44-46]. We suggest that the tumor's inability to properly respond to immunological stimuli, like lipoplexes and/or anti-viral interferons, prevents the tumor tissue from becoming refractory. Our data are consistent with this hypothesis, as tumors from mice pretreated with lipoplexes or IFN-λ show a trend toward increased Doxil® accumulation when compared to PBS treated mice.

The data presented above introduces a novel method of reducing MPS and off-target accumulation of chemotherapeutic nanomedicines. More specifically, our results show that pretreatment with either non-PEGylated lipoplexes or IFN-λ significantly reduces Doxil® accumulation in the major organs of the MPS and other healthy tissues compared to mice pretreated with PBS. Because these MPS organs are predominantly responsible for nanoparticle clearance, even a small decrease in accumulation would allow significantly more particles to remain in circulation. Consistent with this suggestion, our results clearly demonstrate that non-PEGylated lipoplex or IFN-λ pretreatment leads to a significant increase in Doxil® concentrations in the plasma. It is important to recognize that similar effects are not observed when liposomes lacking DNA are used as a pretreatment, indicating that the effects we observe are dependent on the nucleic acid component of the lipoplexes as opposed to saturation of receptors and/or uptake mechanisms. Additionally, our IFN-λ pretreatment mice show almost identical results to non-PEGylated lipoplex treated mice. Moreover, our injections were performed at 24-hour intervals and the uptake mechanisms of the mouse liver are known to be completely regenerated within 3 hours[76]. Taken together, we conclude that MPS saturation by the pretreatment plays no role in the reduction of off-target accumulation. Instead, our results are consistent with the hypothesis that the intravenous administration of lipoplexes elicits an anti-viral response featuring IFN-λ that leads to systemic phenotypic changes that reduce tissue permeability to nano-sized particles.

While interferons generally induce an anti-viral state, they can cause excessive tissue inflammation and damage if left unchecked. However, IFN-λ is unique among the interferon family in that its effects are relatively limited to epithelial/endothelial barriers, such as mucosal and the blood brain barrier, inducing specific and limited functions that minimize unintentional tissue damage[77]. Therefore, this induction of systemic IFN-λ is unlikely to cause detrimental systemic inflammation. Indeed, animals in our studies showed no overt illness or behavioral changes when administered IFN-λ relative to control groups. In this context it is worth noting that a recent clinical trial used subcutaneous IFN-λ injections to reduce viral infections and subsequent hospitalization due to COVID[78]

Interestingly, the lipoplexes we used as a pretreatment for the dextran experiments show significantly different results when used as a pretreatment for Doxil®. We observe increased liver accumulation and decreased plasma concentrations of Doxil® when pretreating with PEGylated lipoplexes. However, when we remove PEG from the lipoplex formulation, we observe the same significant decreases in Doxil® accumulation as we observe with dextran. We hypothesize that using a PEGylated lipoplex as a pretreatment inadvertently primed the immune system against PEG. When a dose of Doxil®, which is heavily PEGylated, is administered 24 hours after a PEGylated lipoplex, an innate immune response to PEG may be initiated, necessitating the exclusion of PEG from the lipoplex formulation.

Considering the immunosuppressed state of the tumor and its muted cytokine response[18, 44-47], we suggested that the IFN-λ-induced phenotypic changes would not be exhibited by the tumor and accumulation would remain unimpeded. As hypothesized, tumors extracted from mice pretreated with IFN-λ exhibit a trend toward increased accumulation and tumor-to-liver ratio of Doxil® per gram of tissue was significantly higher in mice pretreated with IFN-λ. We hypothesize this is due to the significantly higher Doxil® concentration in the plasma of the IFN-λ treated mice and that the ratio may continue to increase with time.

There are several limitations to our study that must be considered when interpreting our results and planning subsequent studies. Only female Balb/c mice were used and only a single CT26 solid tumor model was utilized. Additionally, due to the relatively recent characterization of IFN-λ, there is still much to be elucidated about the exact role of type-III interferons and the mechanisms of actions that IFN-λ propagates. Future studies will need to address the effects of sex, tumor model, and strain/species differences as well as characterize the full extent of the anti-viral immune response to lipoplexes, including type-I interferon production and activation of interferon stimulated genes. The use of a recently developed IFNLR1 deficient mouse model [79] may allow researchers to determine how IFN-λ influences nanomedicine interaction with the body and if blocking IFN-λ or its receptor would be beneficial for gene therapy. We hope that the role of type-III interferons in modifying particle distribution will provide a starting point and inspiration for future studies on the interplay of IFN-λ and nanomedicines.

Conclusions:

In conclusion, our results demonstrate that a lipoplex pretreatment leads to a systemic IFN-λ response that can significantly decrease major organ accumulation of a subsequently

administered particle while simultaneously increasing tumor delivery. Our experimental design avoids contributions from accelerated blood clearance and MPS saturation, and the effects we observe after lipoplex injection are clearly dependent on the inclusion of a nucleic acid component that elicits an IFN-λ response. Furthermore, we demonstrate that direct administration of IFN-λ is also capable of eliciting these effects thereby establishing the role of type-III interferons in regulating particle uptake. Future studies will determine which cell type(s) initiate the IFN-λ response to lipoplexes, which cell type(s) respond to IFN-λ, establish whether an IFN-λ pretreatment can increase the efficacy of Doxil®, and address the clinical relevancy and translational challenges of an IFN-λ pretreatment.

Supplementary Material

Refer to Web version on PubMed Central for supplementary material.

ACKNOWLEDGMENTS:

This work was supported by National Institutes of Health grants R01 GM129046 and K22 AI146141. We are also grateful to Dr. Dmitri Simberg for supplying Doxil® and some of the mice used in our experiments.

Literature Cited.

[1]. Sercombe L, Veerati T, Moheimani F, Wu SY, Sood AK, and Hua S, “Advances and Challenges of Liposome Assisted Drug Delivery” Front Pharmacol, vol. 6, Dec. 2015, doi: 10.3389/fphar.2015.00286.

[2]. Song G, Petschauer JS, Madden AJ, and Zamboni WC, “Nanoparticles and the mononuclear phagocyte system: pharmacokinetics and applications for inflammatory diseases,” Curr Rheumatol Rev, vol. 10, no. 1, pp. 22–34, 2014, doi: 10.2174/1573403x10666140914160554. [PubMed: 25229496]

[3]. Tang Y et al. , “Overcoming the Reticuloendothelial System Barrier to Drug Delivery with a ‘Don’t-Eat-Us’ Strategy,” ACS Nano, vol. 13, no. 11, pp. 13015–13026, Nov. 2019, doi: 10.1021/acsnano.9b05679. [PubMed: 31689086]

[4]. Suk JS, Xu Q, Kim N, Hanes J, and Ensign LM, “PEGylation as a strategy for improving nanoparticle-based drug and gene delivery,” Adv Drug Deliv Rev, vol. 99, no. Pt A, pp. 28–51, Apr. 2016, doi: 10.1016/j.addr.2015.09.012. [PubMed: 26456916]

[5]. Zahednezhad F, Saadat M, Valizadeh H, Zakeri-Milani P, and Baradaran B, “Liposome and immune system interplay: Challenges and potentials,” Journal of Controlled Release, vol. 305, pp. 194–209, Jul. 2019, doi: 10.1016/j.jconrel.2019.05.030. [PubMed: 31121278]

[6]. Abu Lila AS, Kiwada H, and Ishida T, “The accelerated blood clearance (ABC) phenomenon: Clinical challenge and approaches to manage,” Journal of Controlled Release, vol. 172, no. 1, pp. 38–47, Nov. 2013, doi: 10.1016/j.jconrel.2013.07.026. [PubMed: 23933235]

[7]. Mohamed M et al. , “PEGylated liposomes: immunological responses,” Sci Technol Adv Mater, vol. 20, no. 1, pp. 710–724, Jun. 2019, doi: 10.1080/14686996.2019.1627174. [PubMed: 31275462]

[8]. Swartzwelter BJ et al. , “Cross-Species Comparisons of Nanoparticle Interactions with Innate Immune Systems: A Methodological Review,” Nanomaterials (Basel), vol. 11, no. 6, p. 1528, Jun. 2021, doi: 10.3390/nano11061528. [PubMed: 34207693]

[9]. Wiseman JW, Goddard CA, McLelland D, and Colledge WH, “A comparison of linear and branched polyethylenimine (PEI) with DCChol/DOPE liposomes for gene delivery to epithelial cells in vitro and in vivo,” Gene Ther, vol. 10, no. 19, pp. 1654–1662, Sep. 2003, doi: 10.1038/sj.gt.3302050. [PubMed: 12923564]

[10]. Lindberg MF et al. , “Efficient in vivo transfection and safety profile of a CpG-free and codon optimized luciferase plasmid using a cationic lipophosphoramidate in a multiple

intravenous administration procedure," Biomaterials, vol. 59, pp. 1–11, Aug. 2015, doi: 10.1016/j.biomaterials.2015.04.024. [PubMed: 25941996]

[11]. Wilhelm S et al. , "Analysis of nanoparticle delivery to tumours," Nat Rev Mater, vol. 1, no. 5, p. 16014, May 2016, doi: 10.1038/natrevmats.2016.14.

[12]. Lotem M et al. , "Skin Toxic Effects of Polyethylene Glycol–Coated Liposomal Doxorubicin," Arch Dermatol, vol. 136, no. 12, pp. 1475–1480, Dec. 2000, doi: 10.1001/archderm.136.12.1475. [PubMed: 11115157]

[13]. Charrois GJR and Allen TM, "Multiple Injections of Pegylated Liposomal Doxorubicin: Pharmacokinetics and Therapeutic Activity," J Pharmacol Exp Ther, vol. 306, no. 3, pp. 1058–1067, Sep. 2003, doi: 10.1124/jpet.103.053413. [PubMed: 12808004]

[14]. Gabizon A, Shmeeda H, and Barenholz Y, "Pharmacokinetics of Pegylated Liposomal Doxorubicin: Review of Animal and Human Studies," Clinical Pharmacokinetics, vol. 42, no. 5, pp. 419–436, 2003, doi: 10.2165/00003088-200342050-00002. [PubMed: 12739982]

[15]. Wenningmann N, Knapp M, Ande A, Vaidya TR, and Ait-Oudhia S, "Insights into Doxorubicin-induced Cardiotoxicity: Molecular Mechanisms, Preventive Strategies, and Early Monitoring," Mol Pharmacol, vol. 96, no. 2, pp. 219–232, Aug. 2019, doi: 10.1124/mol.119.115725. [PubMed: 31164387]

[16]. Waterhouse DN, Tardi PG, Mayer LD, and Bally MB, "A comparison of liposomal formulations of doxorubicin with drug administered in free form: changing toxicity profiles," Drug Saf, vol. 24, no. 12, pp. 903–920, 2001, doi: 10.2165/00002018-200124120-00004. [PubMed: 11735647]

[17]. Song YK, Liu F, Chu S, and Liu D, "Characterization of Cationic Liposome-Mediated Gene Transfer In Vivo by Intravenous Administration," Human Gene Therapy, vol. 8, no. 13, pp. 1585–1594, Sep. 1997, doi: 10.1089/hum.1997.8.13-1585. [PubMed: 9322091]

[18]. Betker Jamie L. and Anchordoquy Thomas J., "The Effect of Repeat Administration of Lipoplexes on Gene Delivery, Biodistribution, and Cytokine Response in Immunocompetent Tumor-bearing Mice," Journal of Pharmaceutical Sciences, vol. In Press.

[19]. Hyde SC et al. , "CpG-free plasmids confer reduced inflammation and sustained pulmonary gene expression," Nat Biotechnol, vol. 26, no. 5, pp. 549–551, May 2008, doi: 10.1038/nbt1399. [PubMed: 18438402]

[20]. Davies LA et al. , "The use of CpG-free plasmids to mediate persistent gene expression following repeated aerosol delivery of pDNA/PEI complexes," Biomaterials, vol. 33, no. 22, pp. 5618–5627, Aug. 2012, doi: 10.1016/j.biomaterials.2012.04.019. [PubMed: 22575838]

[21]. Li S and Huang L, "In vivo gene transfer via intravenous administration of cationic lipid–protamine–DNA (LPD) complexes," Gene Ther, vol. 4, no. 9, pp. 891–900, Sep. 1997, doi: 10.1038/sj.gt.3300482. [PubMed: 9349425]

[22]. Li S et al. , "Effect of immune response on gene transfer to the lung via systemic administration of cationic lipidic vectors" American Journal of Physiology-Lung Cellular and Molecular Physiology, vol. 276, no. 5, pp. L796–L804, May 1999, doi: 10.1152/ajplung.1999.276.5.L796.

[23]. Ishida T et al. , "Injection of PEGylated liposomes in rats elicits PEG-specific IgM, which is responsible for rapid elimination of a second dose of PEGylated liposomes," J Control Release, vol. 112, no. 1, pp. 15–25, May 2006, doi: 10.1016/j.jconrel.2006.01.005. [PubMed: 16515818]

[24]. Semple SC, Harasym TO, Clow KA, Ansell SM, Klimuk SK, and Hope MJ, "Immunogenicity and Rapid Blood Clearance of Liposomes Containing Polyethylene Glycol-Lipid Conjugates and Nucleic Acid," J Pharmacol Exp Ther, vol. 312, no. 3, pp. 1020–1026, Mar. 2005, doi: 10.1124/jpet.104.078113. [PubMed: 15525796]

[25]. Ishida T and Kiwada H, "Accelerated blood clearance (ABC) phenomenon upon repeated injection of PEGylated liposomes," International Journal of Pharmaceutics, vol. 354, no. 1, pp. 56–62, Apr. 2008, doi: 10.1016/j.ijpharm.2007.11.005. [PubMed: 18083313]

[26]. Kotenko SV et al. , "IFN-λs mediate antiviral protection through a distinct class II cytokine receptor complex," Nature Immunology, vol. 4, no. 1, Art. no. 1, Jan. 2003, doi: 10.1038/ni875. [PubMed: 12496965]

[27]. Mordstein M et al. , "Lambda Interferon Renders Epithelial Cells of the Respiratory and Gastrointestinal Tracts Resistant to Viral Infections," J Virol, vol. 84, no. 11, pp. 5670–5677, Jun. 2010, doi: 10.1128/JVI.00272-10. [PubMed: 20335250]

[28]. Jewell NA et al. , “Lambda Interferon Is the Predominant Interferon Induced by Influenza A Virus Infection In Vivo,” Journal of Virology, vol. 84, no. 21, pp. 11515–11522, Nov. 2010, doi: 10.1128/JVI.01703-09. [PubMed: 20739515]

[29]. Pott J et al. , “IFN-λ determines the intestinal epithelial antiviral host defense,” PNAS, vol. 108, no. 19, pp. 7944–7949, May 2011, doi: 10.1073/pnas.1100552108. [PubMed: 21518880]

[30]. Nice TJ et al. , “Interferon- cures persistent murine norovirus infection in the absence of adaptive immunity,” Science, vol. 347, no. 6219, pp. 269–273, Jan. 2015, doi: 10.1126/science.1258100. [PubMed: 25431489]

[31]. Lazear HM et al. , “Interferon-λ restricts West Nile virus neuroinvasion by tightening the blood-brain barrier,” Sci Transl Med, vol. 7, no. 284, p. 284ra59, Apr. 2015, doi: 10.1126/scitranslmed.aaa4304.

[32]. Miner JJ and Diamond MS, “Mechanisms of restriction of viral neuroinvasion at the blood-brain barrier,” Curr Opin Immunol, vol. 38, pp. 18–23, Feb. 2016, doi: 10.1016/j.coi.2015.10.008. [PubMed: 26590675]

[33]. Galani IE et al. , “Interferon-λ Mediates Non-redundant Front-Line Antiviral Protection against Influenza Virus Infection without Compromising Host Fitness,” Immunity, vol. 46, no. 5, pp. 875–890.e6, May 2017, doi: 10.1016/j.immuni.2017.04.025. [PubMed: 28514692]

[34]. Li L, Xue M, Fu F, Yin L, Feng L, and Liu P, “IFN-Lambda 3 Mediates Antiviral Protection Against Porcine Epidemic Diarrhea Virus by Inducing a Distinct Antiviral Transcript Profile in Porcine Intestinal Epithelia,” Front Immunol, vol. 10, Oct. 2019, doi: 10.3389/fimmu.2019.02394.

[35]. Klinkhammer J et al. , “IFN-λ prevents influenza virus spread from the upper airways to the lungs and limits virus transmission,” eLife, vol. 7, doi: 10.7554/eLife.33354.

[36]. Sommereyns C, Paul S, Staeheli P, and Michiels T, “IFN-Lambda (IFN-λ) Is Expressed in a Tissue-Dependent Fashion and Primarily Acts on Epithelial Cells In Vivo,” PLoS Pathog, vol. 4, no. 3, Mar. 2008, doi: 10.1371/journal.ppat.1000017.

[37]. Swider A, Siegel R, Eskdale J, and Gallagher G, “Regulation of interferon lambda-1 (IFNL1/IFN-λ1/IL-29) expression in human colon epithelial cells,” Cytokine, vol. 65, no. 1, pp. 17–23, Jan. 2014, doi: 10.1016/j.cyto.2013.09.020. [PubMed: 24140069]

[38]. Hermant P and Michiels T, “Interferon-λ in the Context of Viral Infections: Production, Response and Therapeutic Implications,” J Innate Immun, vol. 6, no. 5, pp. 563–574, Aug. 2014, doi: 10.1159/000360084. [PubMed: 24751921]

[39]. Mahlakõiv T, Hernandez P, Gronke K, Diefenbach A, and Staeheli P, “Leukocyte-Derived IFN-α/β and Epithelial IFN-λ Constitute a Compartmentalized Mucosal Defense System that Restricts Enteric Virus Infections,” PLOS Pathogens, vol. 11, no. 4, p. e1004782, Apr. 2015, doi: 10.1371/journal.ppat.1004782. [PubMed: 25849543]

[40]. Odendall C and Kagan JC, “The unique regulation and functions of type III interferons in antiviral immunity,” Curr Opin Virol, vol. 12, pp. 47–52, Jun. 2015, doi: 10.1016/j.coviro.2015.02.003. [PubMed: 25771505]

[41]. Baldridge MT et al. , “Expression of Ifnlr1 on Intestinal Epithelial Cells Is Critical to the Antiviral Effects of Interferon Lambda against Norovirus and Reovirus,” J Virol, vol. 91, no. 7, Mar. 2017, doi: 10.1128/JVI.02079-16.

[42]. Read SA et al. , “Macrophage Coordination of the Interferon Lambda Immune Response,” Front Immunol, vol. 10, Nov. 2019, doi: 10.3389/fimmu.2019.02674.

[43]. Li Y et al. , “Interferon-λ Attenuates Rabies Virus Infection by Inducing Interferon-Stimulated Genes and Alleviating Neurological Inflammation,” Viruses, vol. 12, no. 4, Apr. 2020, doi: 10.3390/v12040405.

[44]. Hanahan D and Weinberg RA, “Hallmarks of Cancer: The Next Generation,” Cell, vol. 144, no. 5, pp. 646–674, Mar. 2011, doi: 10.1016/j.cell.2011.02.013. [PubMed: 21376230]

[45]. Wang D and DuBois RN, “Immunosuppression associated with chronic inflammation in the tumor microenvironment,” Carcinogenesis, vol. 36, no. 10, pp. 1085–1093, Oct. 2015, doi: 10.1093/carcin/bgv123. [PubMed: 26354776]

[46]. Schlößer HA, Theurich S, Shimabukuro-Vornhagen A, Holtick U, Stippel DL, and von Bergwelt-Baildon M, "Overcoming tumor-mediated immunosuppression," Immunotherapy, vol. 6, no. 9, pp. 973–988, Sep. 2014, doi: 10.2217/imt.14.58. [PubMed: 25341119]

[47]. Sindhwani S et al. , "The entry of nanoparticles into solid tumours," Nat. Mater, Jan. 2020, doi: 10.1038/s41563-019-0566-2.

[48]. Betker JL and Anchordoquy TJ, "Non-Additive Effects of Repetitive Administration of Lipoplexes in Immunocompetent Mice," J Pharm Sci, vol. 106, no. 3, pp. 872–881, Mar. 2017, doi: 10.1016/j.xphs.2016.11.013. [PubMed: 27887890]

[49]. Betker JL and Anchordoquy TJ, "Relating Toxicity to Transfection: Using Sphingosine To Maintain Prolonged Expression in Vitro," Mol Pharm, vol. 12, no. 1, pp. 264–273, Jan. 2015, doi: 10.1021/mp500604r. [PubMed: 25418523]

[50]. Betker JL and Anchordoquy TJ, "Effect of charge ratio on lipoplex-mediated gene delivery and liver toxicity," Ther Deliv, vol. 6, no. 11, pp. 1243–1253, 2015, doi: 10.4155/tde.15.77. [PubMed: 26608720]

[51]. Kim Y et al. , "CLEC14A deficiency exacerbates neuronal loss by increasing blood-brain barrier permeability and inflammation," J Neuroinflammation, vol. 17, no. 1, p. 48, Feb. 2020, doi: 10.1186/s12974-020-1727-6. [PubMed: 32019570]

[52]. Guo L et al. , "Vascular Permeability Assay in Human Coronary and Mouse Brachiocephalic Arteries," Bio Protoc, vol. 8, no. 20, p. e3048, Oct. 2018, doi: 10.21769/BioProtoc.3048.

[53]. Liu J, Teng P-Y, Kim WK, and Applegate TJ, "Assay considerations for fluorescein isothiocyanate-dextran (FITC-d): an indicator of intestinal permeability in broiler chickens," Poult Sci, vol. 100, no. 7, p. 101202, Apr. 2021, doi: 10.1016/j.psj.2021.101202. [PubMed: 34111612]

[54]. Chen H, Wu S, Lu R, Zhang Y, Zheng Y, and Sun J, "Pulmonary Permeability Assessed by Fluorescent-Labeled Dextran Instilled Intranasally into Mice with LPS-Induced Acute Lung Injury," PLoS One, vol. 9, no. 7, p. e101925, Jul. 2014, doi: 10.1371/journal.pone.0101925. [PubMed: 25007191]

[55]. Woting A and Blaut M, "Small Intestinal Permeability and Gut-Transit Time Determined with Low and High Molecular Weight Fluorescein Isothiocyanate-Dextrans in C3H Mice," Nutrients, vol. 10, no. 6, p. 685, May 2018, doi: 10.3390/nu10060685. [PubMed: 29843428]

[56]. Pustylnikov S, Sagar D, Jain P, and Khan ZK, "Targeting the C-type Lectins-Mediated Host-Pathogen Interactions with Dextran," J Pharm Pharm Sci, vol. 17, no. 3, pp. 371–392, 2014. [PubMed: 25224349]

[57]. Venturoli D and Rippe B, "Ficoll and dextran vs. globular proteins as probes for testing glomerular permselectivity: effects of molecular size, shape, charge, and deformability," American Journal of Physiology-Renal Physiology, vol. 288, no. 4, pp. F605–F613, Apr. 2005, doi: 10.1152/ajprenal.00171.2004. [PubMed: 15753324]

[58]. Gabizon AA, "Selective Tumor Localization and Improved Therapeutic Index of Anthracyclines Encapsulated in Long-Circulating Liposomes," Cancer Res, vol. 52, no. 4, pp. 891–896, Feb. 1992. [PubMed: 1737351]

[59]. Liu T, Choi H, Zhou R, and Chen I-W, "RES blockade: A strategy for boosting efficiency of nanoparticle drug," Nano Today, vol. 10, no. 1, pp. 11–21, Feb. 2015, doi: 10.1016/j.nantod.2014.12.003.

[60]. Saunders NRM et al. , "A Nanoprimer To Improve the Systemic Delivery of siRNA and mRNA," Nano Lett., vol. 20, no. 6, pp. 4264–4269, Jun. 2020, doi: 10.1021/acs.nanolett.0c00752. [PubMed: 32357299]

[61]. Germain M et al. , "Priming the body to receive the therapeutic agent to redefine treatment benefit/risk profile," Sci Rep, vol. 8, Mar. 2018, doi: 10.1038/s41598-018-23140-9.

[62]. Wan Z et al. , "Mononuclear phagocyte system blockade improves therapeutic exosome delivery to the myocardium," Theranostics, vol. 10, no. 1, pp. 218–230, Jan. 2020, doi: 10.7150/thno.38198. [PubMed: 31903116]

[63]. Ouyang B et al. , "The dose threshold for nanoparticle tumour delivery," Nat. Mater, vol. 19, no. 12, pp. 1362–1371, Dec. 2020, doi: 10.1038/s41563-020-0755-z. [PubMed: 32778816]

[64]. Souhami RL, Patel HM, and Ryman BE, “The effect of reticuloendothelial blockade on the blood clearance and tissue distribution of liposomes,” Biochimica et Biophysica Acta (BBA) - General Subjects, vol. 674, no. 3, pp. 354–371, May 1981, doi: 10.1016/0304-4165(81)90366-4. [PubMed: 6165399]

[65]. Murray IM, “THE MECHANISM OF BLOCKADE OF THE RETICULOENDOTHELIAL SYSTEM,” J Exp Med, vol. 117, no. 1, pp. 139–147, Jan. 1963. [PubMed: 13936766]

[66]. Koenig MG, Heyssel RM, Melly MA, and Rogers DE, “THE DYNAMICS OF RETICULOENDOTHELIAL BLOCKADE,” J Exp Med, vol. 122, no. 1, pp. 117–142, Jul. 1965. [PubMed: 14325467]

[67]. Proffitt RT et al. , “Liposomal Blockade of the Reticuloendothelial System: Improved Tumor Imaging with Small Unilamellar Vesicles” Science, vol. 220, no. 4596, pp. 502–505, Apr. 1983, doi: 10.1126/science.6836294. [PubMed: 6836294]

[68]. Ohara Y et al. , “Effective delivery of chemotherapeutic nanoparticles by depleting host Kupffer cells,” International Journal of Cancer, vol. 131, no. 10, pp. 2402–2410, 2012, doi: 10.1002/ijc.27502. [PubMed: 22362271]

[69]. Wolfram J et al. , “A chloroquine-induced macrophage-preconditioning strategy for improved nanodelivery,” Sci Rep, vol. 7, p. 13738, Oct. 2017, doi: 10.1038/s41598-017-14221-2. [PubMed: 29062065]

[70]. Tavares AJ et al. , “Effect of removing Kupffer cells on nanoparticle tumor delivery,” Proc Natl Acad Sci U S A, vol. 114, no. 51, pp. E10871–E10880, Dec. 2017, doi: 10.1073/pnas.1713390114. [PubMed: 29208719]

[71]. Betker JL et al. , “Nanoparticle Uptake by Circulating Leukocytes: A Major Barrier to Tumor Delivery,” J Control Release, vol. 286, pp. 85–93, Sep. 2018, doi: 10.1016/j.jconrel.2018.07.031. [PubMed: 30030182]

[72]. Dams ETM et al. , “Accelerated Blood Clearance and Altered Biodistribution of Repeated Injections of Sterically Stabilized Liposomes,” J Pharmacol Exp Ther, vol. 292, no. 3, pp. 1071–1079, Mar. 2000. [PubMed: 10688625]

[73]. Yan W, Chen W, and Huang L, “Mechanism of adjuvant activity of cationic liposome: Phosphorylation of a MAP kinase, ERK and induction of chemokines,” Molecular Immunology, vol. 44, no. 15, pp. 3672–3681, Jul. 2007, doi: 10.1016/j.molimm.2007.04.009. [PubMed: 17521728]

[74]. Bila D, Radwan Y, Dobrovolskaia MA, Panigaj M, and Afonin KA, “The Recognition of and Reactions to Nucleic Acid Nanoparticles by Human Immune Cells,” Molecules, vol. 26, no. 14, p. 4231, Jul. 2021, doi: 10.3390/molecules26144231. [PubMed: 34299506]

[75]. Lyass Oet al. , “Correlation of toxicity with pharmacokinetics of pegylated liposomal doxorubicin (Doxil) in metastatic breast carcinoma,” Cancer, vol. 89, no. 5, pp. 1037–1047, 2000, doi: 10.1002/1097-0142(20000901)89:5<1037::AID-CNCR13>3.0.CO;2-Z. [PubMed: 10964334]

[76]. Mates JM et al. , “Mouse Liver Sinusoidal Endothelium Eliminates HIV-Like Particles from Blood at a Rate of 100 Million per Minute by a Second-Order Kinetic Process,” Front. Immunol, vol. 8, Jan. 2017, doi: 10.3389/fimmu.2017.00035.

[77]. Lazear HM, Schoggins JW, and Diamond MS, “Shared and Distinct Functions of Type I and Type III Interferons,” Immunity, vol. 50, no. 4, pp. 907–923, Apr. 2019, doi: 10.1016/j.immuni.2019.03.025. [PubMed: 30995506]

[78]. Reis G et al. , “Early Treatment with Pegylated Interferon Lambda for Covid-19,” N Engl J Med, vol. 388, no. 6, pp. 518–528, Feb. 2023, doi: 10.1056/NEJMoa2209760. [PubMed: 36780676]

[79]. Lin J-Det al. , “Distinct Roles of Type I and Type III Interferons in Intestinal Immunity to Homologous and Heterologous Rotavirus Infections,” PLoS Pathog, vol. 12, no. 4, p. e1005600, Apr. 2016, doi: 10.1371/journal.ppat.1005600. [PubMed: 27128797]

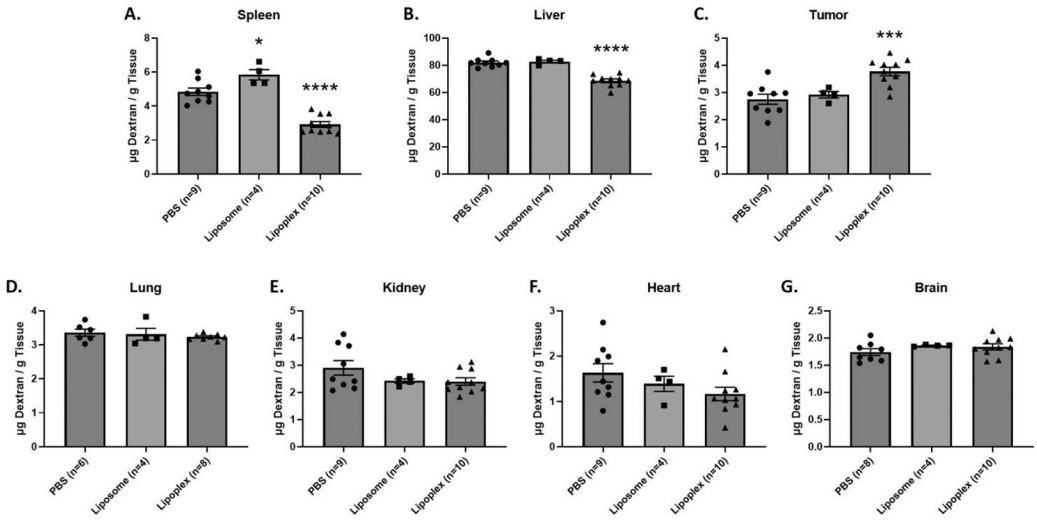

FIGURE 1:

Total dextran accumulation in major organ and tumor tissues. Dextran was administered 24 hours after a 1x PBS, Liposome, or Lipoplex pretreatment injection in Balb/c female mice. Accumulation was measured 24 hours after dextran injection. X-axis represents the pretreatment that the mice received. A t-test with Welch's correction was used to determine if Liposome/Lipoplex pretreatment showed statistically significant differences in accumulation when compared to PBS pretreatment. Statistically significant differences are represented with asterisks (* = $p \leq 0.05$, ** = $p \leq 0.01$, *** = $p \leq 0.001$, **** = $p \leq 0.0001$).

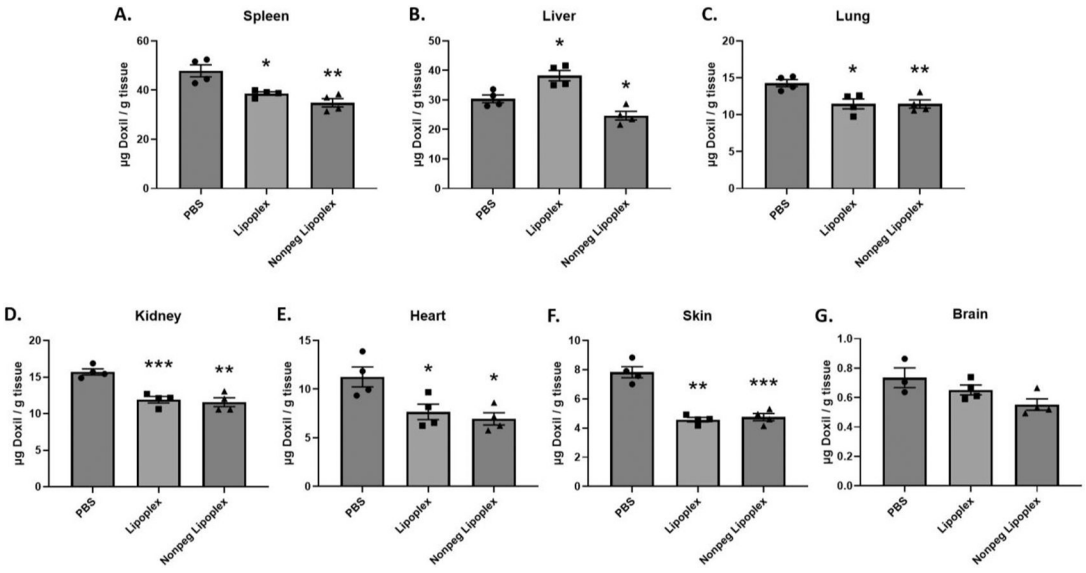

Fig. 2.

Total Doxil® accumulation in major organs. Doxil® was administered 24 h after a 1 × PBS, Lipoplex, or Non-PEGylated Lipoplex pretreatment injection in Balb/c female mice. Accumulation was measured 24 h after Doxil® injection. X-axis represents the pretreatment that the mice received. A *t*-test with Welch's correction was used to determine if Liposome/Lipoplex pretreatment showed statistically significant differences in accumulation when compared to PBS pretreatment. Statistically significant differences are represented with asterisks (* = $p \leq 0.05$, ** = $p \leq 0.01$. *** = $p \leq 0.001$) (A. – F.: $n = 4$) (G.: $n = 3$–4).

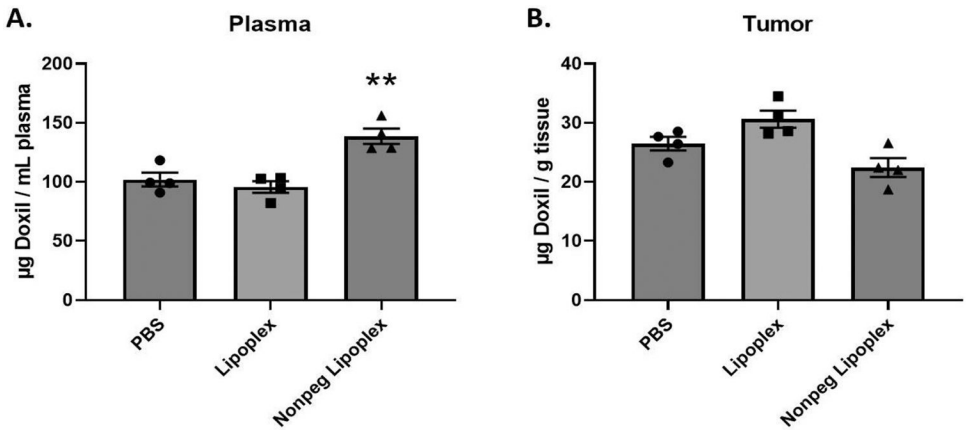

FIGURE 3:

Total Doxil® accumulation in plasma and tumor tissue. Doxil® was administered 24 hours after a 1x PBS, Lipoplex, or Non-PEGylated Lipoplex pretreatment injection in Balb/c female mice. Accumulation was measured 24 hours after Doxil® injection. X-axis represents the pretreatment that the mice received. A t-test with Welch's correction was used to determine if Liposome/Lipoplex pretreatment showed statistically significant differences in accumulation when compared to PBS pretreatment. Statistically significant differences are represented with asterisks (* = $p \leq 0.05$, ** = $p \leq 0.01$) (A. – B.: n = 4).

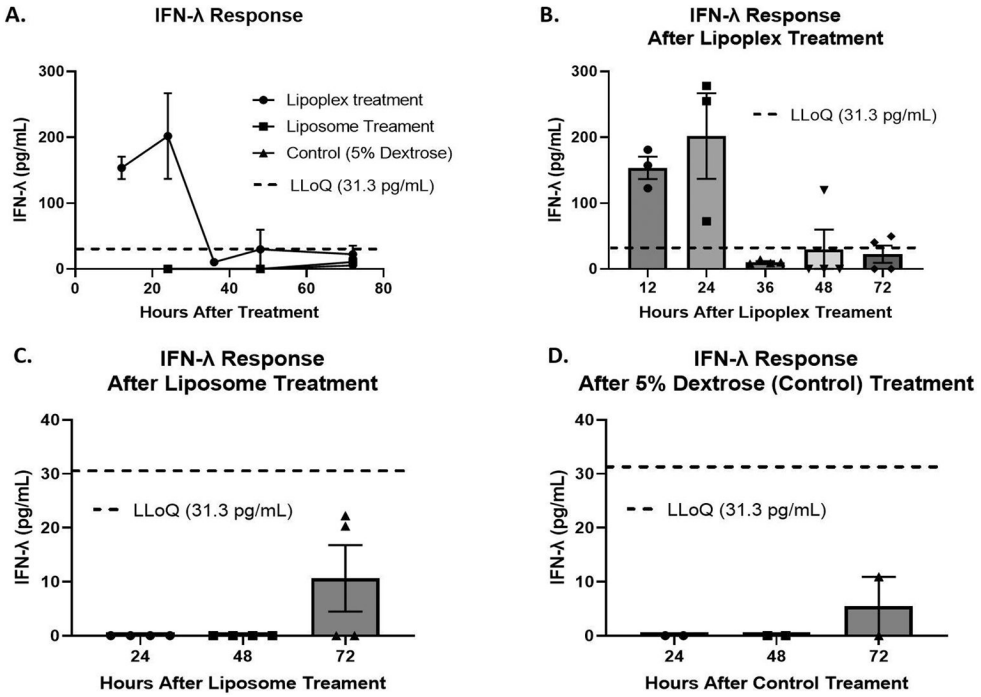

FIGURE 4:

A: Quantification of IFN-λ in serum of Balb/c female mice after lipoplex, liposome, and 5% dextrose treatment using ELISA. B: Quantification of IFN-λ in serum of mice after lipoplex treatment C: Quantification of IFN-λ in serum of mice after liposome treatment D: Quantification of IFN-λ in serum of mice after 5% dextrose (control) treatment. Error bars represent the mean and the standard error of the mean. Lower limit of quantification (LLoQ) of ELISA: 31.3 pg/mL. Lower limit of detection (LLoD) of ELISA: 3.9 pg/mL. Lipoplex treatment n = 3 – 4. Liposome treatment n = 4. Control treatment n = 2.

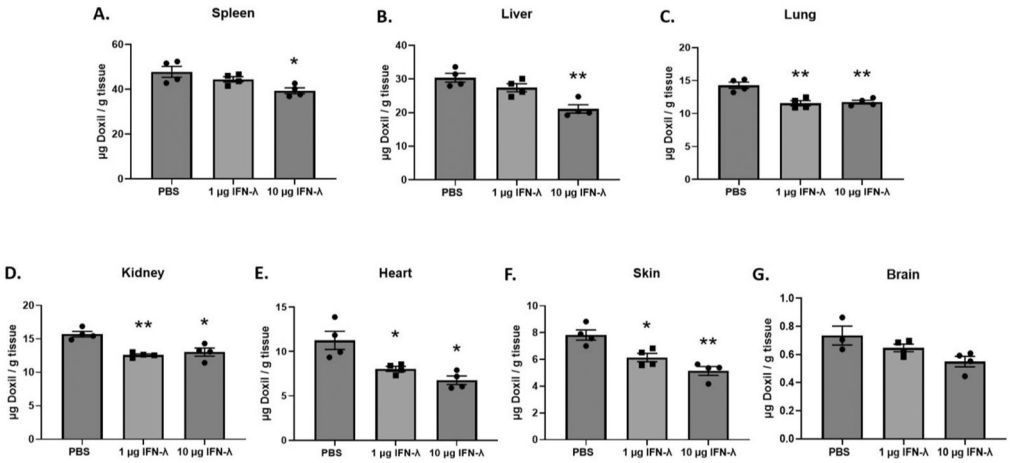

FIGURE 5:

Total Doxil® accumulation in major organs. Doxil® was administered 24 hours after a 1x PBS, 1 µg IFN-λ, or 10 µg IFN-λ pretreatment injection in Balb/c female mice. Accumulation was measured 24 hours after Doxil® injection. X-axis represents the pretreatment that the mice received. A t-test with Welch's correction was used to determine if IFN-λ pretreatment showed statistically significant differences in accumulation when compared to PBS pretreatment. Statistically significant differences are represented with asterisks (* = $p \leq 0.05$, ** = $p \leq 0.01$, *** = $p \leq 0.001$) (A. – F.: n = 4) (G.: n = 3 – 4).

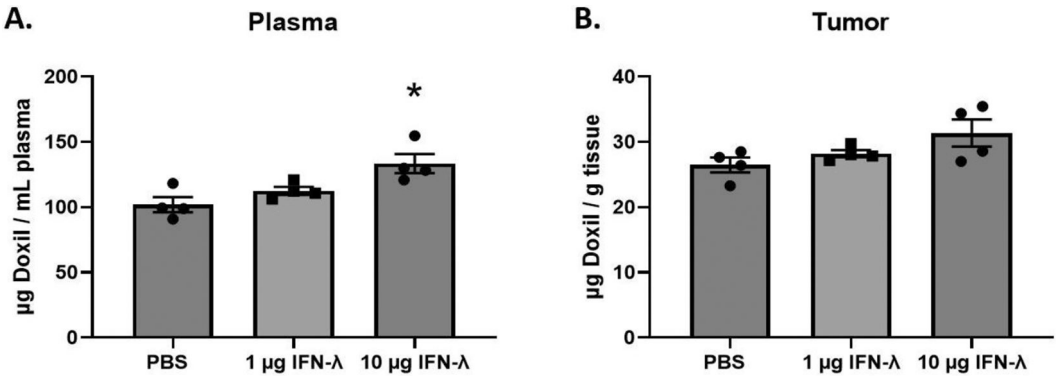

Fig. 6.

Total Doxil® accumulation in plasma and tumor tissue. Doxil® was administered 24 h after a 1× PBS. 1 µg IFN-λ, or 10 µg IFN-λ pretreatment injection in Balb/c female mice. Accumulation was measured 24 h after Doxil® injection. X-axis represents the pretreatment that the mice received. A *t*-test with Welch's correction was used to determine if IFN-λ pretreatment showed statistically significant differences in accumulation when compared to PBS. Statistically significant differences are represented with asterisks (* = $p \leq 0.05$) (A. – B.: $n = 4$).

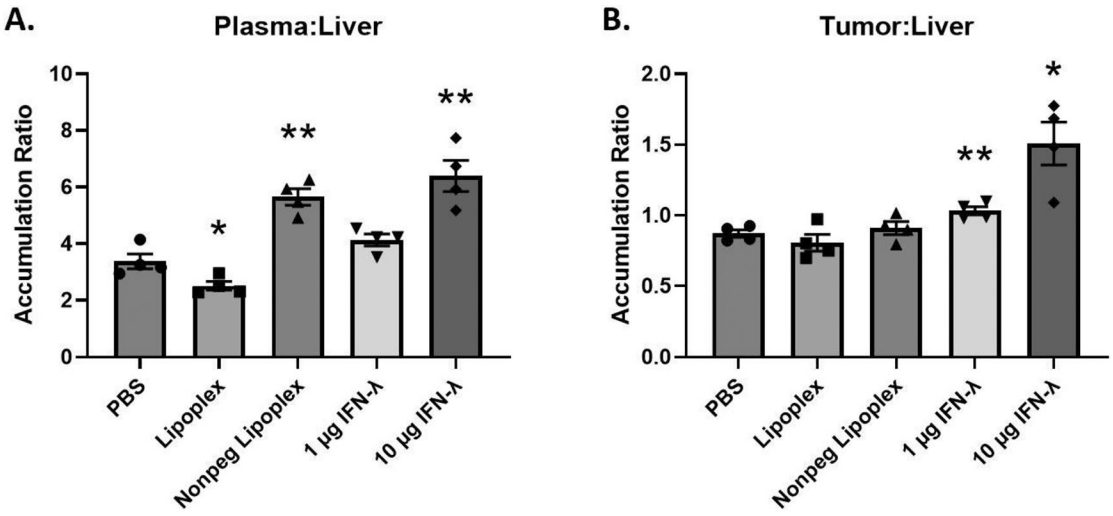

Figure 7:

Plasma/liver and tumor/liver Doxil accumulation ratios. X-axis represents the pretreatment that the mice received. A t-test with Welch's correction was used to determine if Lipoplex and IFN-λ pretreatments showed statistically significant differences in accumulation ratios when compared to PBS pretreatment. Statistically significant differences are represented with asterisks (* = $p \leq 0.05$, ** = $p \leq 0.01$) (A. – B.: n = 4).